

The role of spatial scale in joint optimisations of generation and transmission for European highly renewable scenarios

Jonas Hörsch, Tom Brown

Frankfurt Institute for Advanced Studies, Ruth-Moufang-Straße 1, 60438 Frankfurt am Main, Germany

Email: hoersch@fias.uni-frankfurt.de

Abstract—The effects of the spatial scale on the results of the optimisation of transmission and generation capacity in Europe are quantified under a 95% CO₂ reduction compared to 1990 levels, interpolating between one-node-per-country solutions and many-nodes-per-country. The trade-offs that come with higher spatial detail between better exposure of transmission bottlenecks, exploitation of sites with good renewable resources (particularly wind power) and computational limitations are discussed. It is shown that solutions with no grid expansion beyond today's capacities are only around 20% more expensive than with cost-optimal grid expansion.

I. INTRODUCTION

Optimising investment in the electricity system to reduce greenhouse gas emissions is computationally intensive. Transmission investment should be jointly optimised with generation investment, so that the benefits of exploiting the sites with the best renewable resources can be balanced against the network expansion costs; continental-scale areas should be considered, so that synoptic-scale weather variations (~600-1000 km), which particularly affect wind generation, can be balanced; at the same time, high spatial detail is required to capture both variations in renewable resources and existing transmission bottlenecks.

Previous studies have typically sacrificed at least one of these goals. In some studies, only a single node per country or group of countries has been considered [1]–[4], ignoring national transmission networks and local differences in weather conditions. Other studies consider the transmission network in detail, but only for single countries [5], [6], neglecting the benefits of international cooperation. Other studies maintain both a pan-continental scope and transmission network detail, but fix the generation fleet and only optimise the transmission network [7], [8].

In this paper it is attempted to bring a more systematic approach to the question of spatial resolution in electricity system optimisations. A clustering methodology called ‘*k*-means’ is used to successively reduce the number of nodes in the European transmission network from its full level of spatial detail down to a level where there is only one node per country. The effects on the results of the optimal investments in generation and transmission are then studied as the spatial resolution is changed. A high spatial resolution reveals transmission bottlenecks that might either restrict

welfare-enhancing transfers or force transmission upgrades; ignoring these effects in a low resolution model leads to an underestimate of the total costs. In a low resolution model one is also forced to average the renewable resources over a larger area, which lowers the average capacity factors, even with a weighting towards better sites; at high resolution the sites with the highest capacity factors can be fully exploited, particularly for wind.

In recent decades as large-scale optimisation has gained in importance, many methods have been suggested in the literature to reduce the whole network to a number of clusters, rather than focussing on a binary exterior-interior division like the Ward or Radial-Equivalent-Independent methods [9]. Standard clustering algorithms from complex network theory [10] have been applied on the network structure, including *k*-means clustering [11] on electrical distance between buses [12]–[14] and spectral partitioning of the Laplacian matrix [15]. Equivalents based on zonal Power Transfer Distribution Factors (PTDFs) were considered in [16], while a methodology based on Available Transfer Capacities (ATCs) was developed in [17]. A more economic focus was taken in [18], where buses were clustered based on similar average locational marginal price (LMP). The final report of the recent e-Highways 2050 project [19] that considered network expansion needs in Europe contains both a summary of network clustering methods and suggestions for mixed metrics combining several characteristics to define nodal similarity.

In the following sections we review the clustering methodology, the investment model, the data input for the European electricity system and the results for different aggregation scales and levels of grid expansion.

II. METHODOLOGY FOR NETWORK REDUCTION

We first describe the method to derive a clustered equivalent network, with fewer buses and lines, from a more detailed network. First, the network buses are partitioned into clusters, then an equivalent network is constructed with one bus per cluster and aggregated lines between the new buses.

The network reduction method used here for an equivalent network of *k* buses consists of the following steps:

- 1) Univalent buses, i.e. network stubs or ‘dead-ends’, are aggregated to their neighbours in an iterative process

until all buses are multi-valent, since such stubs are typically short lines, connecting single generators to the main network.

- 2) The remaining buses labelled by n are assigned a weight w_n proportional to the load and today's conventional generation capacities at the bus and coordinates x_n based on their geographical location.
- 3) The k -means algorithm is used to find the geographical positions of k centroids $\{x_c\}$ for $c = 1, \dots, k$ by minimising the weighted sum of squared distances from each centroid to its clustered members N_c :

$$\min_{\{x_c\}} \sum_{c=1}^k \sum_{n \in N_c} w_n \|x_c - x_n\|^2 \quad (1)$$

To lessen the risk of finding local minima the k -means algorithm is run on 10 different starting conditions and all but the best found centroid configuration are discarded. Further, the clustering is constrained so that for each country and synchronous zone a number of clusters proportional to its overall mean load is chosen.

- 4) A new bus c is created at each centroid x_c to represent the set of clustered nodes.
- 5) All generators, storage units and loads that were connected to the original buses in N_c are then aggregated by technology type at the equivalent bus c . The maximum expansion potential of generators of the same technology type are added for the new aggregated generator, while the weather-dependent availability time series for renewable generators are averaged with a weighting.
- 6) Lines between the clusters are replaced by a single equivalent line with a length of 1.25 times the crow-flies-distance, whose capacity is given by the sum of the capacity of the replaced lines, and whose impedance is given by the equivalent impedance of the parallel lines.

Note that by focussing on the geographical distribution of the load and conventional generation, this method ignores both the electrical distance between the buses and the grid topology. Electrical distance is ignored because the network clustering should be independent of existing grid capacities, given that these capacities will be optimised later; for the optimisation, geographical distance is more important because it determines the cost of the grid expansion. The topology is ignored because it is expected that the grid topology was designed to connect major load and conventional generation centres, so that focussing on the load and generation is sufficient to capture the important conglomerations and the transmission corridors between them.

N-1 security is modelled by scaling down the available transmission capacity to 0.7 times nominal capacity for high resolution networks ≥ 200 clusters and linearly shrinking it down until reaching half the nominal values at 37 clusters to account for cluster-internal bottlenecks.

The network model is clustered down to $k = 37, 45, 64, 90, 128, 181, 256, 362$ buses (see Figure 2 for the clusterings with 64 and 362 buses) and the different results of the system optimisation are examined for each level of clustering in several grid expansion scenarios.

The network reduction algorithms are implemented in the free software 'Python for Power System Analysis (PyPSA)' Version 0.8.0 [20], which is developed at the Frankfurt Institute for Advanced Studies (FIAS). PyPSA uses the scikit-learn Python package [21] for the k -means clustering.

III. MODEL FOR INVESTMENT OPTIMISATION

The model minimises total annual system costs, which include the variable and fixed costs of generation, storage and transmission, given technical and physical constraints.

To obtain a representative selection of weather and demand conditions while keeping computation times reasonable, the model is run over every third hour of a full historical year of weather and demand data assuming perfect foresight, with 2012 chosen as the representative year. Each time point t is weighted by $w_t = 3$ in the objective function and storage constraints, to account for the fact that it represents three hours.

The optimisation minimises total annual system costs, with objective function

$$\min_{G_{n,s}, F_\ell, g_{n,s,t}, f_{\ell,t}} \left[\sum_{n,s} c_{n,s} G_{n,s} + \sum_{\ell} c_\ell F_\ell + \sum_{n,s,t} w_t o_{n,s} g_{n,s,t} \right] \quad (2)$$

consists of the capacities $G_{n,s}$ at each bus n for generation and storage technologies s and their associated annualised fixed costs $c_{n,s}$, the dispatch $g_{n,s,t}$ of the unit in time t and the associated variable costs $o_{n,s}$, and the line capacities F_ℓ for each line ℓ (including both high voltage alternating current (HVAC) and direct current (HVDC) lines) and their annualised fixed costs c_ℓ .

The dispatch of conventional generators $g_{n,s,t}$ is constrained by their capacity $G_{n,s}$

$$0 \leq g_{n,s,t} \leq G_{n,s} \quad \forall n, s, t \quad (3)$$

The maximum producible power of renewable generators depends on the weather conditions, which is expressed as an availability $\bar{g}_{n,s,t}$ per unit of its capacity:

$$0 \leq g_{n,s,t} \leq \bar{g}_{n,s,t} G_{n,s} \quad \forall n, s, t \quad (4)$$

The energy levels $e_{n,s,t}$ of all storage units have to be consistent between all hours and are limited by the storage energy capacity $E_{n,s}$

$$\begin{aligned} e_{n,s,t} &= \eta_0^t e_{n,s,t-1} - \eta_1 w_t [g_{n,s,t}]^- + \eta_2^{-1} w_t [g_{n,s,t}]^+ \\ &\quad + w_t g_{n,s,t,\text{inflow}} - w_t g_{n,s,t,\text{spillage}} \\ 0 &\leq e_{n,s,t} \leq E_{n,s} \quad \forall n, s, t \end{aligned} \quad (5)$$

Positive and negative parts of a value are denoted as $[\cdot]^+ = \max(\cdot, 0)$, $[\cdot]^- = -\min(\cdot, 0)$. The storage units can have a standing loss η_0 , a charging efficiency η_1 , a discharging efficiency η_2 , inflow (e.g. river inflow in a reservoir) and spillage. The energy level is assumed to be cyclic, i.e. $e_{n,s,t=0} = e_{n,s,t=T}$.

CO₂ emissions are limited by a cap CAP_{CO_2} , implemented using the specific emissions e_s in CO₂-tonne-per-MWh of the fuel s and the efficiency $\eta_{n,s}$ of the generator:

$$\sum_{n,s,t} \frac{1}{\eta_{n,s}} w_t g_{n,s,t} \cdot e_s \leq \text{CAP}_{\text{CO}_2} \quad \leftrightarrow \quad \mu_{\text{CO}_2} \quad (6)$$

In all simulations this cap was set at a reduction of 95% of the electricity sector emissions from 1990.

The (inelastic) electricity demand $d_{n,t}$ at each bus n must be met at each time t by either local generators and storage or by the flow $f_{\ell,t}$ from a transmission line ℓ

$$\sum_s g_{n,s,t} - d_{n,t} = \sum_{\ell} K_{n\ell} f_{\ell,t} \quad \forall n, t \quad (7)$$

where $K_{n\ell}$ is the incidence matrix of the network. This equation is essentially Kirchhoff's Current Law (KCL).

In this paper it is assumed that the linear load flow is a good approximation for a well-compensated transmission network [8], [22]. To guarantee the physicality of the network flows, in addition to KCL, Kirchhoff's Voltage Law (KVL) must be enforced in each connected network. KVL states that the voltage differences around any closed cycle in the network must sum to zero. If each independent cycle c is expressed as a directed combination of lines ℓ by a matrix $C_{\ell c}$ then KVL becomes the constraint

$$\sum_{\ell} C_{\ell c} x_{\ell} f_{\ell,t} = 0 \quad \forall c, t \quad (8)$$

where x_{ℓ} is the series inductive reactance of line ℓ . Note that point-to-point HVDC lines have no cycles, so there is no constraint on their flow beyond KCL.

The flows are also constrained by the line capacities F_{ℓ}

$$|f_{\ell,t}| \leq F_{\ell} \quad \forall \ell, t \quad (9)$$

Although the capacities F_{ℓ} are subject to optimisation, no new grid topologies are considered.

Since line capacities F_{ℓ} can be continuously expanded to represent the addition of new circuits, the impedances x_{ℓ} of the lines would also decrease. In principle this would introduce a bilinear coupling in equation (8) between the x_{ℓ} and the $f_{\ell,t}$. To keep the optimisation problem linear and therefore computationally fast, x_{ℓ} is left fixed in each optimisation problem, updated and then the optimisation problem is rerun in up to 4 iterations to ensure convergence, following the methodology of [23].

In order to investigate the interactions of spatial scale with transmission expansion, the sum of all transmission line capacities (HVAC and HVDC) multiplied by their lengths l_{ℓ} is restricted by a line volume cap CAP_{trans} , which is then varied in different simulations:

$$\sum_{\ell} l_{\ell} \cdot F_{\ell} \leq CAP_{\text{trans}} \quad \leftrightarrow \quad \mu_{\text{trans}} \quad (10)$$

The caps are defined in relation to today's line capacities F_{ℓ}^{today} , i.e.

$$CAP_{\text{trans}} = x \cdot CAP_{\text{trans}}^{\text{today}} = x \cdot \sum_{\ell} l_{\ell} \cdot F_{\ell}^{\text{today}}. \quad (11)$$

The discussion in Section V starts off with the no expansion scenario, $CAP_{\text{trans}} = CAP_{\text{trans}}^{\text{today}}$ so that no network expansion is possible beyond today's line capacities. In this scenario transmission bottlenecks restrict the exploitation of the best renewable sites and the smoothing effects across the continent; generation is forced to be more localised and renewable

TABLE I
INVESTMENT COSTS

Quantity	Overnight Cost [€]	Unit	FOM [%/a]	Lifetime [a]
Wind onshore	1182	kW _{el}	3	20
Wind offshore	2506	kW _{el}	3	20
Solar PV	600	kW _{el}	4	20
Gas	400	kW _{el}	4	30
Battery storage	1275	kW _{el}	3	20
Hydrogen storage	2070	kW _{el}	1.7	20
Transmission line	400	MWkm	2	40

variability may have to be balanced by storage. Then, five expansion scenarios are studied by gradually easing the cap $CAP_{\text{trans}} = x \cdot CAP_{\text{trans}}^{\text{today}}$ with $x = 1.125, 1.25, 1.5, 2, 3$ until reaching three times today's transmission volume, which is already above the optimal value for overhead lines at high numbers of clusters, as we will discuss in Section V-B.

The optimisation model was also implemented in PyPSA.

IV. DATA INPUTS

The network reduction and subsequent investment optimisation were run on a full model of the European electricity transmission system.

The existing network capacities and topology for the ENTSO-E area (including continental Europe, Scandinavia, the Baltic countries, Great Britain and Ireland) were taken from the GridKit extraction [24] of the online ENTSO-E Interactive Transmission Map [25]. The model includes all transmission lines with voltages above 220 kV and all HVDC lines in the ENTSO-E area (see Figure 1). In total the model contains 5586 HVAC lines with a volume of 241.3 TWkm (of which 11.4 TWkm are still under construction), 26 HVDC lines with a volume of 3.4 TWkm (of which 0.5 TWkm are still under construction) and 4653 substations.

The hourly electricity demand profiles for each country in 2012 are taken from the European Network of Transmission System Operators for Electricity (ENTSO-E) website [26]. The geographical distribution of load in each country is based on GDP and population statistics for the NUTS3 regions.

Electricity generation in the model is allowed from the following technologies: hydroelectricity, natural gas, solar PV, onshore wind and offshore wind. Gas, solar and wind capacities may be expanded within the model constraints.

Existing hydroelectricity capacities (including run-of-river, reservoirs and pumped storage) were compiled by matching databases CARMA [27], GEO [28], DOE Global Energy Storage Database [29] and the PowerWatch project coordinated by the World Resources Institute [30]; no expansion of existing hydro capacities is considered in the model. The hydro energy storage capacities are based on country-aggregated data reported by [31], [32] and the inflow time series are provided by [31].

The only fossil fuel generators in the model are open cycle gas turbines, whose efficiency is assumed to be 39%. Their usage is limited by the CO₂ cap in equation (6).

The potential generation time series for wind and solar generators are computed with the Aarhus renewable energy

atlas [33] from hourly historical weather data from 2012 with a spatial resolution of $40 \times 40 \text{ km}^2$ provided by the US National Oceanic and Atmospheric Administration [34].

The distribution of these generators is proportional to the quality of each site given by the local capacity factor multiplied with the maximum installable capacity of the site. However, protected sites as listed in Natura2000 [35] are excluded, as well as areas with certain land use types from the Corine Land Cover database [36], as specified by [2], to avoid building, e.g., wind turbines in urban areas. The maximum water depths for offshore wind turbines is assumed to be 50 m. The maximum installable capacity per bus and generator type is then determined by scaling these layouts until the first site reaches a maximum installation density of 2 and 1.7 MW/km² for wind and solar, respectively. These maximum densities are chosen conservatively to take account of competing land use and minimum-distance regulations for onshore wind turbines.

The model contains two extendable types of storage units: batteries and hydrogen storage. Their charging and discharging efficiencies, as well as cost assumptions for their power and energy storage capacities are taken from [37]. It is assumed that the charging and discharging power capacities of a unit are equal, and the energy capacity $E_{n,s} = h_{max,s} * G_{n,s}$ is proportional to this power capacity. The factor $h_{max,s}$ determines the time for charging or discharging the storage completely at maximum power, and is set to $h_{max} = 6 \text{ h}$ for batteries and to 168 h for H2 storage.

Investment and fixed operation and maintenance (FOM) costs for all assets are listed in Table I. The costs for generating assets are based on predictions for 2030 from DIW [38]; the costs for battery and hydrogen electricity storage power capacity and energy storage capacity come from [37]. Although the costs of lines c_ℓ are set to zero, as they are dual to the line volume cap, these costs are added in afterwards in the results. For the annualisation of overnight costs a discount rate of 7% is used. Gas variable costs add up to 21.6 €/MWh_{th}[38].

V. RESULTS

The original European grid model is shown in Figure 1 and can be compared to two clustered networks in Figure 2; the total annual system costs in the three scenarios as a function of the number of clusters is found in Figure 4 and these costs are broken down into components in Figure 3; the expansion of the transmission network is shown in further detail in Figure 5; the system costs as a function of the transmission cap are plotted in Figure 6; finally the shadow price of the transmission cap can be studied in Figure 7. The results of the scenarios are now discussed in detail.

A. Spatial scale dependence

Without any expansion of the transmission network ($x = 1.0$ in Figure 4), the total annual system cost remains approximately steady as the number of clusters increases at 260 billion euros (an average of around € 82/MWh), due to a coincidental balance of the two driving effects: (1) The sites with high capacity factors are more finely resolved with a higher number

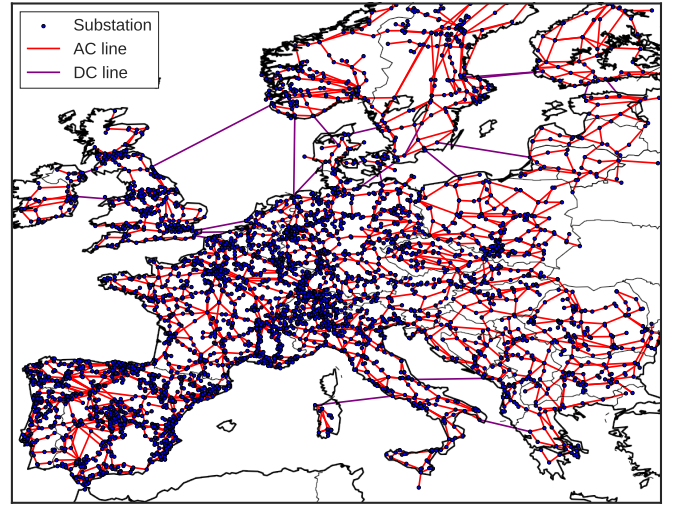


Fig. 1. Original grid model of Europe, described at the beginning of Sec. IV

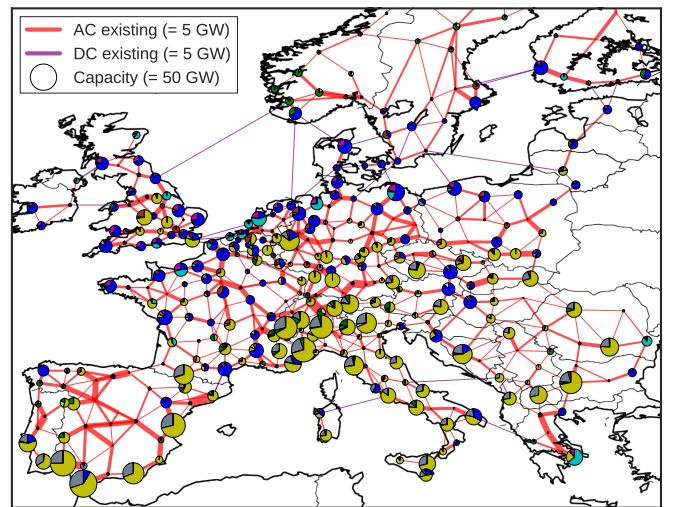
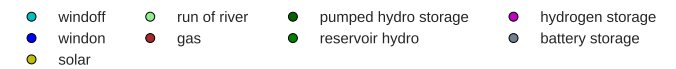
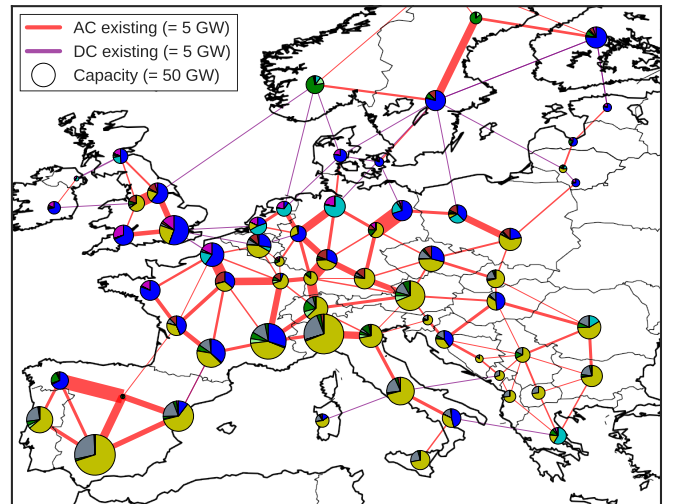


Fig. 2. The clusterings with 64 buses (above) and 362 buses (below). Results for the distribution of generation capacities at each node are shown as pie charts for the no expansion scenario (existing and planned projects only).

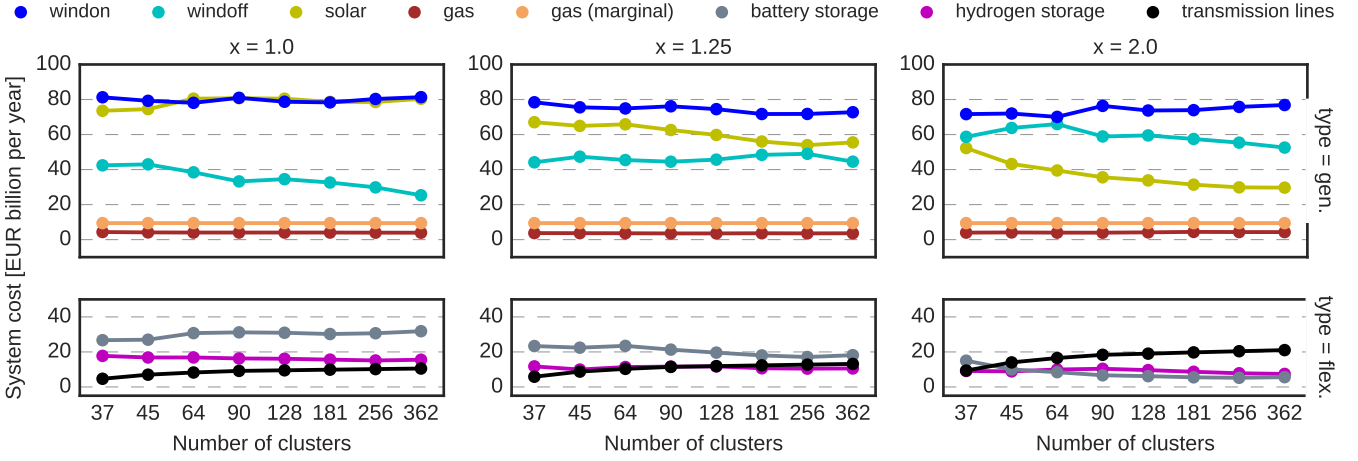


Fig. 3. Breakdown of the annual system costs for generation (top) and flexibility options (bottom) as a function of the number of clusters for the no expansion scenario and the expansion scenarios with $x = 1.25$ and $x = 2$.

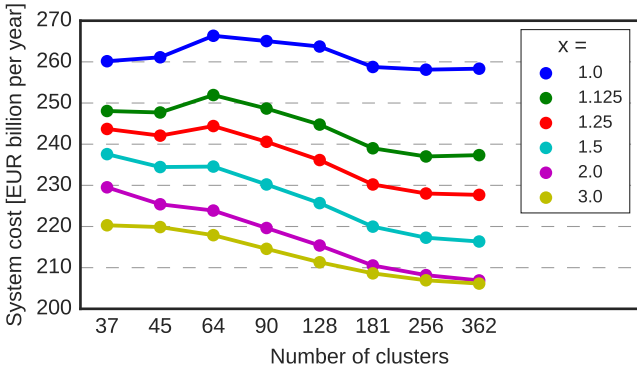


Fig. 4. Total annual system costs as a function of the number of clusters for the six scenarios including the costs for overhead transmission lines.

of clusters, allowing the model to put more capacity at the best sites. With smaller numbers of clusters, the capacity factors are averaged with a weighting over a larger area, bringing the capacity factors down. For example, the best cluster for onshore wind in Germany with 362 clusters has a capacity factor of about 40 %, whereas with one node for the whole of Germany, the weighted average capacity factor is only 26 %. (2) As the number of clusters increases, the bottlenecks inside each country's network become constraining and prevent the wind generated at high capacity factors, localised on the coastlines and offshore, to be transported to load centres.

In the left panel in Figure 3, the two effects, the increasing effective capacity factor of onshore wind combined with intra-country bottlenecks becoming more important, lead to the considerable decrease in the built offshore wind capacity, since better sited onshore wind and solar installations produce more energy closer to the load. The increasing solar generation drives an increase in battery capacities to smooth short-term diurnal variability. Hydrogen storage, which balances longer-term synoptic and seasonal variability, decreases gently with the number of clusters at a higher level than the other two sce-

narios. Gas generation is fixed because of the CO_2 constraint. The grid costs increase monotonically as more line capacity and line constraints are seen by the model, but flatten out with the exponentially increasing number of clusters. This is a good indication that the clustering is capturing the major transmission corridors even with smaller numbers of clusters.

Turning back to Figure 4, the expansion of the network lifts transmission bottlenecks and the first effect wins out, better exploitation of good sites with higher numbers of clusters decrease the system cost. As the grid is gradually expanded the system cost decreases in a very non-linear manner: The expansion by 25% reduces the total system cost already by 30 billion euros of the 50 billion euros in cost reduction available down to 210 billion euros (an average of € 66/MWh). Nevertheless the overall cost reduction possible by expanding the network is a moderate 20%.

In the technology break-down in the center and right panels of Figure 3, with the additional line volume the joint solar and battery capacities are replaced by offshore wind turbines. Solar is favoured with limited transmission capacity because it can be built close to demand everywhere and reasonably balanced during its principal short-term diurnal variation using battery storage, whereas the good wind sites are concentrated in Northern Europe and their energy cannot be transported to loads in large quantities without an expansion of the transmission grid. Wind generation additionally benefits from expanding the transmission capacities so that the spatial variation on the continental scale is used for smoothing the temporal fluctuations on the synoptic scale to relieve expensive hydrogen storage. The extra transmission capacity does not offset the low significance of the transmission network cost.

These trends are all pronounced if the results for Germany are considered in isolation. Transmission bottlenecks within Germany complicate transporting offshore wind energy away from the coast with higher numbers of clusters, forcing a dramatic substitution by solar instead, i.e. the German offshore wind capacity falls from 40 GW to 12 GW from 37 to 362 clusters, while solar peak capacities increase from 46 GW to

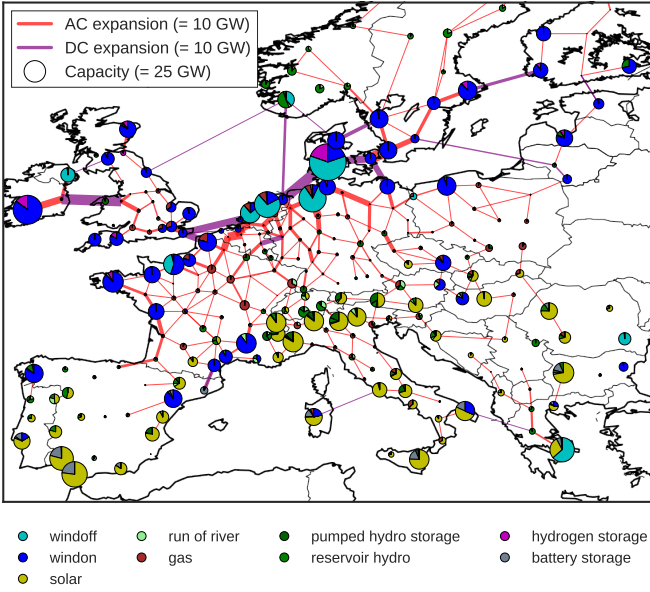


Fig. 5. Optimal generation capacities and transmission line expansion for 256 buses in the expansion scenario with the transmission cap at $x = 2$.

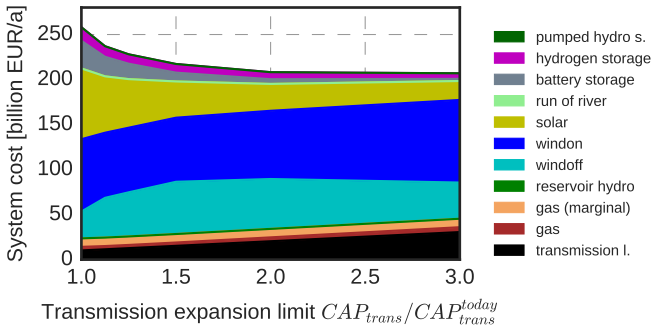


Fig. 6. Annual total system cost at 256 clusters for different values of the transmission cap CAP_{trans} .

100 GW and onshore wind remains largely unaffected despite an intermediate decrease.

The effects disappear for about 200 clusters and above, a level of resolution above which all the results are more-or-less steady.

B. Transmission volume cap

After ensuring that the solutions have already stabilized at 200 clusters and are thus, likely, a good proxy for the relations on the full network, we want to focus in more detail on the solutions for 256 clusters while varying the allowed overall transmission volume to find the most important lines for expansion and estimate the benefits of a partial expansion deviating from the optimal solution, which might be preferable vis-à-vis problems of public acceptance.

Figure 5 shows the optimal generation capacities and transmission expansion for a challenging doubling of the existing transmission capacity ($x = 2$), which was also the subject of the right panel in Figure 3. Transmission is foremost expanded in the proximity of wind capacity installations forming a wide

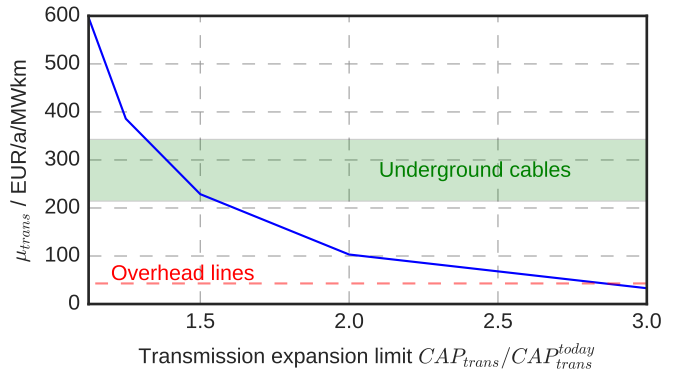


Fig. 7. Shadow price of the line volume constraint μ_{trans} for different values of the transmission cap CAP_{trans} for 256 clusters.

band along the shore of the north and east sea with branches leading inland. This band allows synoptic-scale balancing as weather systems pass from west to east over Europe. It provides the flexibility for the energy of large-scale wind installations to replace a significant amount of solar capacity in Southern Europe and Italy in particular, which also lessens the need for short-term battery storage.

The total system cost in respect to allowed transmission volume in Figure 6 decreases non-linearly as has already been observed in the detailed study in the one-node-per-country setting by Schlachtberger et. al [4]. More than half of the overall benefit of transmission of 50 billion EUR per year is already locked in at an expansion by a fourth to $1.25 \cdot CAP_{trans}^{today}$ and after reaching two times today's line volume ($x = 2$) does not increase significantly anymore (also compare the vertical slice at 256 clusters in Figure 4). From a system constrained to today's transmission capacities to the optimal solution, the cost composition reduces the component spent on solar and battery in favour of offshore wind and, then, also onshore wind.

Finally, the shadow price of the transmission cap, μ_{trans} introduced in Equation (10) is shown in Figure 7. It indicates the marginal value of an increase in line volume at each level of network expansion; it can also be interpreted as the transmission line cost per MWkm necessary for the optimal solution to have the transmission line volume CAP_{trans} . For the assumed costs for over-land transmission lines of 400 €/MWkm the model finds the optimal grid volume at slightly below $3 \cdot CAP_{trans}^{today}$. If the expansion instead were to be carried out with underground cabling at a 4 to 8 times higher cost, the economically optimal solution would still be to expand the line volume to between 1.25 and 1.5 times the existing volume.

VI. CRITICAL APPRAISAL

Although the clustering algorithm presented in Section II captures the major transmission corridors well, it would be interesting to benchmark the different clustering algorithms mentioned in the introduction based on comparable criteria, such as their ability to capture power flows in the original unclustered network. Results with a higher number of nodes would also be desirable, if this is computationally possible.

Additional aspects, such as distribution grid costs, reserve power, stability and sector-coupling, have not been considered here.

VII. DISCUSSION AND CONCLUSIONS

The results of this paper are two fold: Firstly, a network clustering method has been demonstrated that can reduce the number of buses in a given electricity network while maintaining the major transmission corridors for network analysis. With this network reduction method the effects of spatial resolution, i.e. the number of clusters, on the joint optimisation of transmission and generation investment for highly renewable systems in Europe have been investigated. Secondly, the techno-economic European model was optimised at a sufficient level of resolution to determine the hotspots and benefits of transmission expansion.

The systems optimised to reduce CO₂ emissions by 95% with no grid expansion are consistently only around 20% more expensive than systems with grid expansion and half of that cost benefit can already be locked in with an expansion of the line volume by a fourth, which may be a price worth paying given public acceptance problems for new transmission lines.

One must note, though, that in the time horizon until 2050 in which the studied reduction of emissions is to be implemented a significant amount of the current conventional generation park will not yet have passed their lifetime and an important next step is to confirm our greenfield results accounting for this inertia. Further, one should be clear that the feasibility of these solutions is based on a fully integrated European market with nodal prices, high CO₂ price and optimally real-time prices for distributed generation and storage.

ACKNOWLEDGMENTS

This research was conducted as part of the CoNDyNet project, which is supported by the German Federal Ministry of Education and Research under grant no. 03SF0472C. The responsibility for the contents lies solely with the authors.

REFERENCES

- [1] G. Czisch, "Szenarien zur zukünftigen Stromversorgung," PhD thesis, Universität Kassel, 2005.
- [2] Y. Scholz, "Renewable energy based electricity supply at low costs - Development of the REMix model and application for Europe," PhD thesis, Universität Stuttgart, 2012. DOI: 10.18419/opus-2015.
- [3] Rodriguez, R.A., Becker, S., Andresen, G., Heide, D., and Greiner, M., "Transmission needs across a fully renewable European power system," *Renewable Energy*, vol. 63, pp. 467–476, 2014.
- [4] D. Schlachtberger, T. Brown, S. Schramm, and M. Greiner, "The benefits of cooperation in a highly renewable european electricity network," *Energy*, 2017, accepted. arXiv: 1704.05492.
- [5] "Kombikraftwerk 2: Abschlussbericht," Fraunhofer IWES et al., Tech. Rep., Aug. 2014. [Online]. Available: <http://www.kombikraftwerk.de/mediathek/abschlussbericht.html>.
- [6] C. Nabe, "Impacts of restricted transmission grid expansion in a 2030 perspective in germany," in *Wind Integration Workshop, Berlin*, 2014.
- [7] Egerer, J., Lorenz, C., and Gerbaulet, C., "European electricity grid infrastructure expansion in a 2050 context," in *10th International Conference on the European Energy Market*, IEEE, 2013, pp. 1–7. DOI: 10.1109/EEM.2013.6607408.
- [8] Brown, T., Schierhorn, P., Tröster, E., and Ackermann, T., "Optimising the European transmission system for 77% renewable electricity by 2030," *IET Renewable Power Generation*, vol. 10, no. 1, pp. 3–9, 2016. DOI: 10.1049/iet-rpg.2015.0135.
- [9] S. Deckmann, A. Pizzolante, A. Monticelli, B. Stott, and O. Alsac, "Studies on power system load flow equivalencing," *IEEE Transactions on Power Apparatus and Systems*, vol. PAS-99, no. 6, pp. 2301–2310, Nov. 1980, ISSN: 0018-9510. DOI: 10.1109/TPAS.1980.319798.
- [10] A. K. Jain, M. N. Murty, and P. J. Flynn, "Data clustering: A review," *ACM Comput. Surv.*, vol. 31, no. 3, pp. 264–323, Sep. 1999, ISSN: 0360-0300. DOI: 10.1145/331499.331504.
- [11] J. A. Hartigan and M. A. Wong, "Algorithm AS 136: A K-means clustering algorithm," *Applied Statistics*, vol. 28, no. 1, pp. 100–108, 1979.
- [12] H. Temraz, M. Salama, and V. Quintana, "Application of partitioning techniques for decomposing large-scale electric power networks," *International Journal of Electrical Power & Energy Systems*, vol. 16, no. 5, pp. 301–309, 1994, ISSN: 0142-0615. DOI: 10.1016/0142-0615(94)90034-5.
- [13] S. Blumsack, P. Hines, M. Patel, C. Barrows, and E. C. Sanchez, "Defining power network zones from measures of electrical distance," in *2009 IEEE Power Energy Society General Meeting*, Jul. 2009, pp. 1–8. DOI: 10.1109/PES.2009.5275353.
- [14] E. Cotilla-Sanchez, P. D. H. Hines, C. Barrows, S. Blumsack, and M. Patel, "Multi-attribute partitioning of power networks based on electrical distance," *IEEE Transactions on Power Systems*, vol. 28, no. 4, pp. 4979–4987, Nov. 2013, ISSN: 0885-8950. DOI: 10.1109/TPWRS.2013.2263886.
- [15] C. Hamon, E. Shayesteh, M. Amelin, and L. Söder, "Two partitioning methods for multi-area studies in large power systems," *International Transactions on Electrical Energy Systems*, vol. 25, no. 4, pp. 648–660, 2015, ETEP-12-0480.R1, ISSN: 2050-7038. DOI: 10.1002/etep.1864.
- [16] X. Cheng and T. J. Overbye, "PTDF-based power system equivalents," *IEEE Transactions on Power Systems*, vol. 20, no. 4, pp. 1868–1876, Nov. 2005, ISSN: 0885-8950. DOI: 10.1109/TPWRS.2005.857013.
- [17] E. Shayesteh, B. F. Hobbs, L. Söder, and M. Amelin, "ATC-Based System Reduction for Planning Power Systems With Correlated Wind and Loads," *IEEE Transactions on Power Systems*, vol. 30, no. 1, pp. 429–438, Jan. 2015, ISSN: 0885-8950.

- [18] H. K. Singh and S. C. Srivastava, "A reduced network representation suitable for fast nodal price calculations in electricity markets," in *IEEE Power Engineering Society General Meeting, 2005*, Jun. 2005, 2070–2077 Vol. 2. DOI: 10.1109/PES.2005.1489092.
- [19] "EHighways 2050 Final Reports," ENTSO-E et al., Tech. Rep., 2015. [Online]. Available: <http://www.e-highway2050.eu/>.
- [20] T. Brown, J. Hörsch, and D. Schlachtberger, *PyPSA: Python for Power System Analysis Version 0.8.0*. 2017. DOI: 10.5281/zenodo.582307. [Online]. Available: <http://pypsa.org/>.
- [21] F. Pedregosa, G. Varoquaux, A. Gramfort, V. Michel, B. Thirion, O. Grisel, M. Blondel, P. Prettenhofer, R. Weiss, V. Dubourg, J. Vanderplas, A. Passos, D. Cournapeau, M. Brucher, M. Perrot, and E. Duchesnay, "Scikit-learn: Machine learning in Python," *Journal of Machine Learning Research*, vol. 12, pp. 2825–2830, 2011.
- [22] B. Stott, J. Jardim, and O. Alsac, "DC power flow revisited," *IEEE Trans. Power Syst.*, vol. 24, no. 3, p. 1290, 2009. DOI: 10.1109/TPWRS.2009.2021235.
- [23] Hagspiel, S., Jägemann, C., Lindener, D., Brown, T., Cherevatskiy, S., and Tröster, E., "Cost-optimal power system extension under flow-based market coupling," *Energy*, vol. 66, pp. 654–666, 2014.
- [24] B. Wiegmanns, *GridKit extract of ENTSO-E interactive map*, Jun. 2016. DOI: 10.5281/zenodo.55853.
- [25] *ENTSO-E Interactive Transmission System Map*, Jan. 2016. [Online]. Available: <https://www.entsoe.eu/map/>.
- [26] *Country-specific hourly load data*, 2012. [Online]. Available: <https://www.entsoe.eu/data/data-portal/consumption/>.
- [27] K. Ummel, "CARMA revisited: An updated database of carbon dioxide emissions from power plants worldwide," *Center for Global Development Working Paper*, no. 304, 2012.
- [28] Rajan Gupta, Harihar Shankar et. al., *Global energy observatory*, 2016. [Online]. Available: <http://globalenergyobservatory.org/> (visited on 09/2016).
- [29] Sandia National Laboratories, *DOE Global Energy Storage Database*, 2016. [Online]. Available: www.energystorageexchange.org/projects (visited on 09/2016).
- [30] World Resources Institute, *PowerWatch: An open-source global power plant database project*, 2016. [Online]. Available: <https://github.com/Arjay7891/WRI-Powerplant> (visited on 09/2016).
- [31] Kies, A., Chattopadhyay, K., von Bremen, L., Lorenz, E., and Heinemann, D., "RESTORE 2050 Work Package Report D12: Simulation of renewable feed-in for power system studies.," RESTORE 2050, Tech. Rep., 2016, in preparation.
- [32] B. Pflüger, F. Sensfuß, G. Schubert, and J. Leisenritt, "Tangible ways towards climate protection in the european union (eu long-term scenarios 2050)," *Fraunhofer ISI*, 2011.
- [33] G. B. Andresen, A. A. Søndergaard, and M. Greiner, "Validation of Danish wind time series from a new global renewable energy atlas for energy system analysis," *Energy*, vol. 93, Part 1, pp. 1074–1088, 2015. DOI: 10.1016/j.energy.2015.09.071.
- [34] S. et al., "The ncep climate forecast system reanalysis," *Bull. Amer. Meteor. Soc.*, vol. 91, no. 8, pp. 1015–1057, 2010.
- [35] EEA, *Natura 2000 data - the european network of protected sites*, 2016. [Online]. Available: <http://www.eea.europa.eu/data-and-maps/data/natura-7>.
- [36] —, *Corine land cover (clc) 2012, version 18.5.1*, 2012. [Online]. Available: <http://land.copernicus.eu/pan-european/corine-land-cover/clc-2012/view>.
- [37] C. Budischak, D. Sewell, H. Thomson, L. Mach, D. E. Veron, and W. Kempton, "Cost-minimized combinations of wind power, solar power and electrochemical storage, powering the grid up to 99.9% of the time," *Journal of Power Sources*, vol. 225, pp. 60–74, 2013, ISSN: 0378-7753. DOI: 10.1016/j.jpowsour.2012.09.054.
- [38] A. Schröder, F. Kunz, J. Meiss, R. Mendelevitch, and C. von Hirschhausen, "Current and prospective costs of electricity generation until 2050," eng, Deutsches Institut für Wirtschaftsforschung (DIW), Berlin, Data Documentation, DIW 68, 2013.